DEVELOPMENT OF A CLICK CHEMISTRY APPROACH FOR CANCER CELL TARGETING AND EVALUATING THE EFFECT OF PROTEIN CORONA ON ACTIVE TARGETING YIELD

BY

VAHID MIRSHAFIEE

THESIS

Submitted in partial fulfillment of the requirements
for the degree of Master of Science in Chemical Engineering
in the Graduate College of the
University of Illinois at Urbana-Champaign, 2013

Urbana, Illinois

Adviser:

Assistant Professor Mary L. Kraft

ABSTRACT

The routine approach for targeting nanoparticle delivery vehicles to cancer cells is by incorporating targeting ligands (e.g. antibodies or aptamers) to the surface of nanoparticles (NPs). Although targeting ligands are known to interact with specific receptors in the membranes of cancer cells, resulting in enhanced NP uptake, these functionalized NPs have an undesirable biodistribution and unfavorable targeting efficacy. Here we demonstrate a novel approach to target NPs to the cancer cells via click chemistry. Cancer cells are first metabolically labeled with an azide-modified monosaccharide (azidosugar). In the second step, NPs that are functionalized with highly-reactive cycloalkynes selectively bind to the cancer cells due to a spontaneous click reaction between the cycloalkynes on NP's surfaces and the metabolically incorporated azide groups in the cell membranes. Our results show that HeLa and Chinese hamster ovary (CHO) cells are successfully labeled with azidosugars, and cycloalkyne-functionalized silica NPs bind to the metabolically labeled cells via the click reaction.

The click chemistry reaction was also used to study the effect of protein adsorption on active NP targeting. Upon exposure of NPs to the biological environment, proteins and other biomolecules bind to the NPs and cover their surfaces. This protein coating, which is called the protein corona, may reduce the targeting capability of functionalized NPs by screening their targeting ligands. Here we used cycloalkyne-functionalized silica NPs that can bind to the azide-modified silicon substrates to study this effect. The results demonstrate that the formation of protein corona significantly decreased the conjugation of functionalized NPs to the substrate.

ACKNOWLEDGEMENTS

I would like to gratefully thank Prof. Mary Kraft for her tremendous supervision and mentoring. I sincerely appreciate your encouragement and supportive guidance during this research. Your valuable support helped me to develop my scientific skills and prepare myself for my future career. In addition, I thank Prof. Jianjun Cheng in Materials Science and Engineering Department at University of Illinois at Urbana-Champaign and Prof. Morteza Mahmoudi in the Department of Nanotechnology, Faculty of Pharmaceutics at Tehran University of Medical Sciences for their great help regarding this project.

I also thank Kraft group members, Dr. Kaiyan Lou, Rayna Kim, Haley Klitzing, and Dr. Robbie Wilson. I would like to also thank Cheng group members, Dr. Li Tang and Qian Yin.

Finally, I sincerely thank my beloved family for their great support and encouragement throughout my life.

TABLE OF CONTENTS

CHAPTER 1. INTRODUCTION

1.1 Cancer and Drug Delivery

Cancer is one of the leading causes of death in the United States and many other parts of the word such that 25% of deaths in the United States are due to cancer.[1] Among current approaches for cancer treatment, anti-cancer drugs can significantly inhibit the tumor growth, but they have undesired side effects, such as toxicity toward healthy tissues. In addition to these side effects, multiple administrations of the anticancer drug are typically required to maintain an effective drug concentration in the body (Figure 1.1). Consequently, new drug delivery approaches are required to overcome these obstacles.

Nanoparticles are a promising delivery system for specifically targeting anticancer drugs to tumors, thereby reducing their detrimental side effects.[2] Drug-loaded nanoparticles may have the ability to deliver drugs to a desired location in the body and release the drug over long periods of time with a maintained concentration. This would improve the therapeutic activity of the drug, reduce the number of required drug administrations, and yield a less invasive cancer treatment.

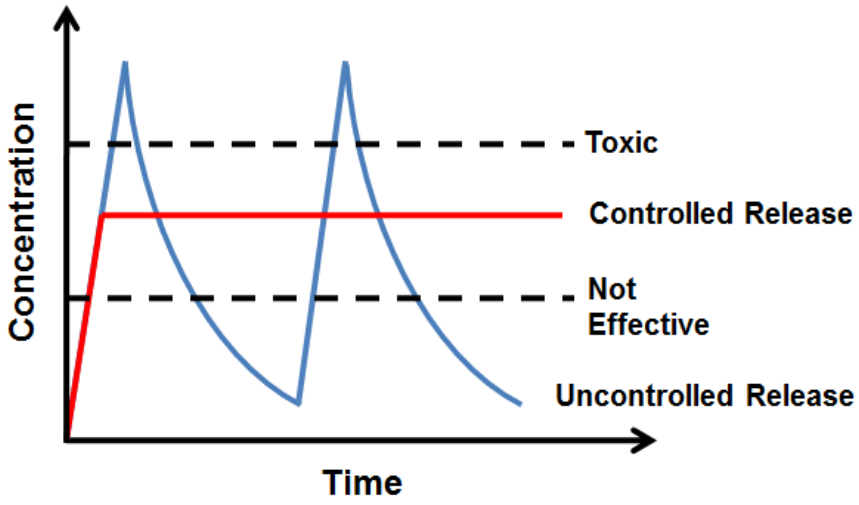

Figure 1.1. Plot shows the drug concentration in the body as a function of time for a traditional drug delivery system (i.e., a pill or injection) and a controlled release system. The controlled release system maintains a constant drug concentration that is within the therapeutic window (the area between dashed lines). In contrast, for the traditional non-controlled drug delivery system, the drug concentration rapidly rises into toxic levels shortly after administration, and then drops to ineffective levels as the time interval increases, necessitating multiple administrations.

For targeting nanoparticles to cancer cells, nanoparticles should pass through spleen, liver and kidney filtration and diffuse to the tumor tissue. Passive targeting is a common tumor targeting approach that exploits the defective tumor vasculature that makes the blood vessels surrounding tumors more permeable than normal tissue, which is called the enhanced permeability and retention (EPR) effect.[3] Thus, nanomaterials with a specific size range, around 10 nm to 100 nm,[3] can pass through this leaky vasculature and accumulate in tumor tissue (Figure 1.2).[4]

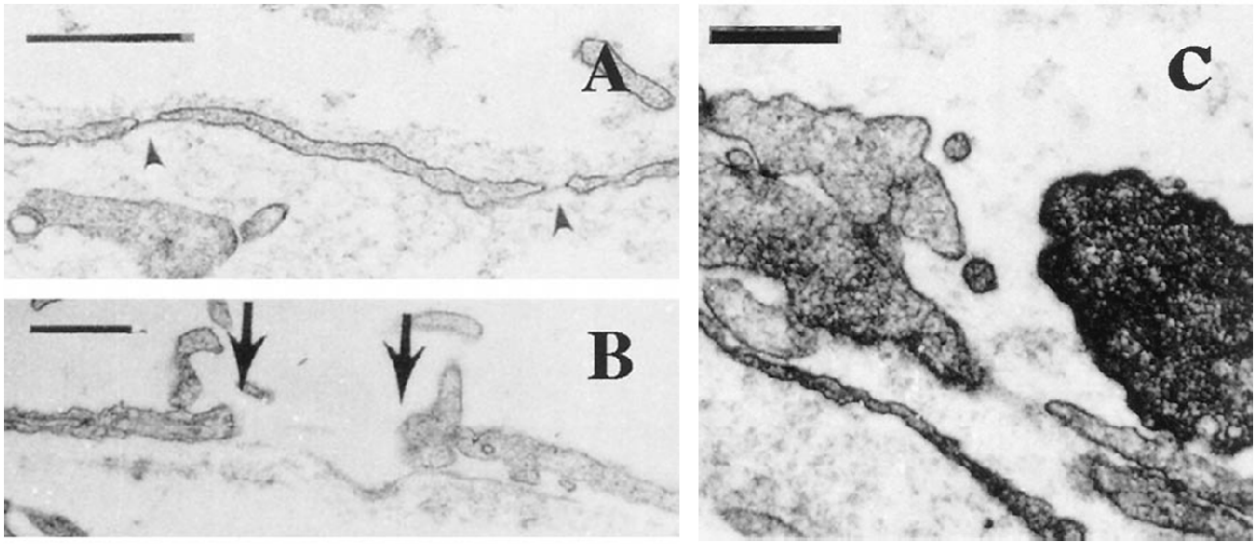

Figure 1.2. Electron micrograph showing permeable structure of tumor blood vessels (Copyright (1998) National Academy of Sciences, U.S.A., Ref 4).

An active nanoparticle targeting method has also been developed to increase the overall accumulation of nanoparticles in cancer cells in order to increase their therapeutic efficacy. For active targeting, the surface of nanoparticle is functionalized with small molecules, called targeting ligands (*e.g.* antibodies or aptamers), which selectively interact with receptors in the cancer cell's plasma membrane, leading to nanoparticle's uptake by the cancer cells (Figure 1.3).[2,5] Nanoparticles that are functionalized with active targeting ligands still exploit the EPR effect in order to penetrate into the tumor tissue, but their binding to the cancer cell's surface is expected to enhance their uptake. Unfortunately, active targeting approaches seldom achieved significant improvements in targeting efficiency *in vivo*. A large fraction of the nanoparticles accumulate in the liver and spleen instead of the tumor,[6] and the circulation time of nanoparticles

that are modified with targeting ligands is lower than unmodified nanoparticles.[7] These factors prohibit the effective *in vivo* targeting of NP-ligand conjugates, resulting in an increased immune response and reduced anticancer efficacy.[7] Thus, fundamental changes in the design of NPs for cancer targeting are urgently needed to overcome this unfavorable biodistribution.

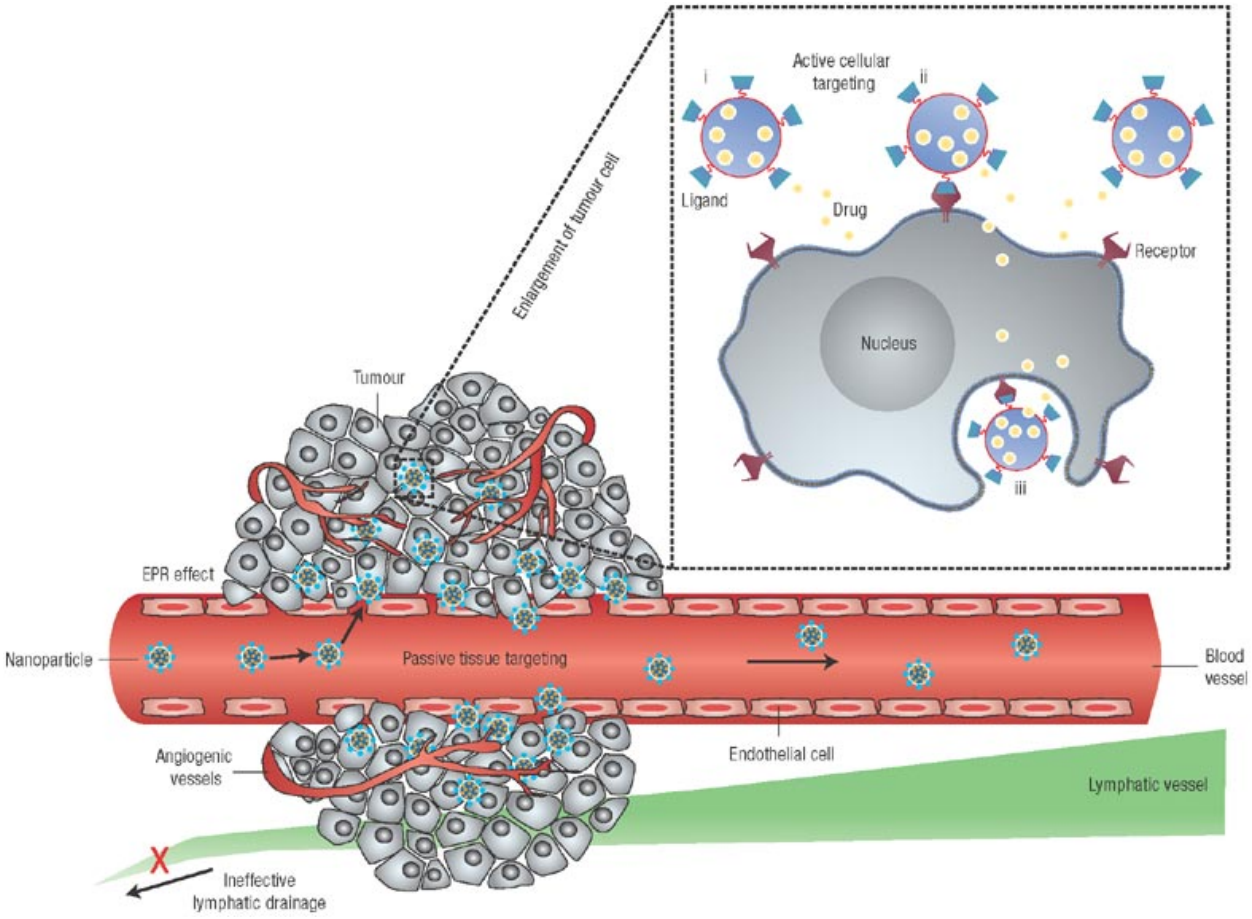

Figure 1.3. Passive and active targeting of nanoparticles to the tumor (Reprinted by permission from Macmillan Publishers Ltd: [Nature Nanotechnology] (Ref.2), copyright (2007)).

1.2 Protein Corona

When NPs are exposed to biological fluids within the *in vivo* environment, proteins and other biomolecules adsorb to their surface. The resulting protein coating, which is named the protein corona,[8-10] is stable for several hours. Previous studies show that the protein corona can significantly influence NP's uptake by the cells. For example, Lesniak et al. have shown that the protein adsorption to the NPs' surfaces decreases cellular uptake.[11] A study of cellular uptake of

silica NPs in the presence and absence of the protein corona indicates the protein corona reduces cellular uptake and alters the NPs' intracellular locations.[12] The protein corona may also affect NPs targeting efficacy by a non-biological mechanism. When nanoparticles are functionalized with targeting ligands and applied *in vivo*, the proteins and biomolecules that absorb to the NP's surface may cover the targeting ligands, preventing them from interacting with their target receptors in the plasma membranes of the cancer cells. The protein corona's hindrance effect may lead to a low targeting yield for functionalized NPs *in vivo*. Thus, investigating this effect can help researchers to design more efficient targeted delivery methods.

1.3 Click Chemistry and Metabolic Labeling of Glycans

Glycans are oligosaccharide moieties attached to lipids and proteins. Glycans are involved in important biological processes such as cell adhesion[13] and cancer progression.[14] In fact, changes in glycans structure signal a change in the cell's physiological condition.[15] The ability to image glycans might permit detecting these health-related changes. However, unlike proteins, glycans cannot be labeled with genetically encoded probes, which renders the detection and imaging of glycans significantly more challenging. To address this challenge, Prof. C. R. Bertozzi and co-workers have developed a two-step method for imaging glycans that is based on click chemistry.[16,17] Click chemistry is defined as a modular reaction that occurs in very high yield and generates only inoffensive byproducts that are easily removed.[18] For imaging glycans in cells, this click chemistry reaction must be compatible with physiological conditions. Therefore, this reaction must be rapid and high-yielding when performed in an aqueous environment at physiological temperature. In addition, the click chemistry reactants must be bioorthogonal, which means they selectively react with each other, but not with the chemical moieties that are native to biomolecules.

The click reaction between azides and cycloalkynes has been widely used to label biological components.[19] Because the azide group is small, mammalian cells can metabolize monosaccharides that are modified with an azide (X in Figure 1.4), and incorporate these modified sugars into their glycans.[16,17] In the two-step glycan imaging method developed by Prof. C. R. Bertozzi and co-workers, the cells are first metabolically labeled with an azide-modified sugar, which is called an azidosugar (Figure 1.4).[16,17] In the second step, a click chemistry reaction occurs between the metabolically incorporated azidosugars on the cells and

reactive cycloalkyne moieties that are attached to fluorescent probes, which enables imaging the glycans with fluorescence microscopy.[16,17]

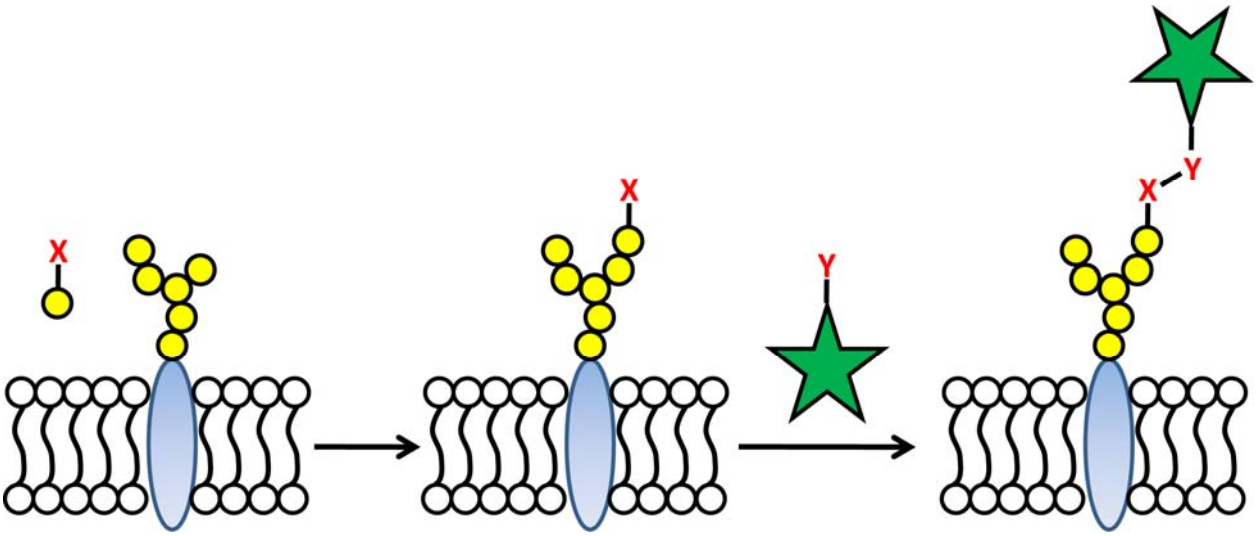

Figure 1.4. Metabolic labeling of glycans on the cell membrane

The most employed click reactions with azides include copper catalyzed cycloadditions with terminal alkynes, modified Staudinger ligations with phosphines, and strain-promoted cycloadditions with cyclooctynes (Scheme 1.1).[19] Unfortunately, the copper catalyst that is required for the cycloaddition of azides with terminal alkynes is toxic to cells, which is undesirable for cell labeling experiments.[19-21] The bioorthogonal reaction between azide group and phosphines, known as Staudinger ligation, is a popular copper-free click reaction that could be used in biological systems.[22,23] However, the utility of this reaction for *in vivo* studies is limited by its slow reaction kinetics.[19] Fortunately, the strain-promoted cycloaddition reaction between azides and cyclooctynes achieves the desired rapid reaction kinetics without the use of a toxic catalyst.[19] Moreover, adding an electron-withdrawing fluorine to the cyclooctyne moiety drastically increases the rate of the cycloaddition with an azide.[24,25]

In the past decade, the click chemistry reaction between an azide and a strained alkyne has been used to selectively label and image glycans in numerous reported studies.[19] Here we summarize a few studies that are relevant to the subject of this thesis. In a study carried out by the Bertozzi research group, glycans of a developing zebrafish were imaged by using a difluorinated cyclooctyne (DIFO).[15] They have successfully detected differences in the cell-surface expression of glycans, their intracellular trafficking, and tissue distribution via this

metabolic labeling and copper-free click chemistry approach.[15] The Bertozzi group has also investigated the labeling efficiency as a function of cyclooctyne structure.[26] In this study, mouse cells were metabolically labeled by the introduction of N-azidoacetylmannosamine (Ac_4ManNAz), and then various cyclooctynes with different side groups were injected to the mice to investigate their labeling efficiency.[26] The results revealed that although some cyclooctynes reacted with modified glycans on the cells surface, the amount of protein binding, which was influenced by the lipophilicity of the cyclooctyne, reduced the targeting and labeling efficiency.[26,27] Unfortunately, the synthesis of the stained cycloalkynes used in this study, such as DIFO, is very time consuming and involves numerous (>8) sequential reactions. To address this drawback, Dommerholt et al. developed a new cyclooctyne, called a bicyclononyne (BCN), which has sufficient reactivity toward azides for click reactions, can be synthesized in far fewer steps, and also has less protein binding affinity.[27]

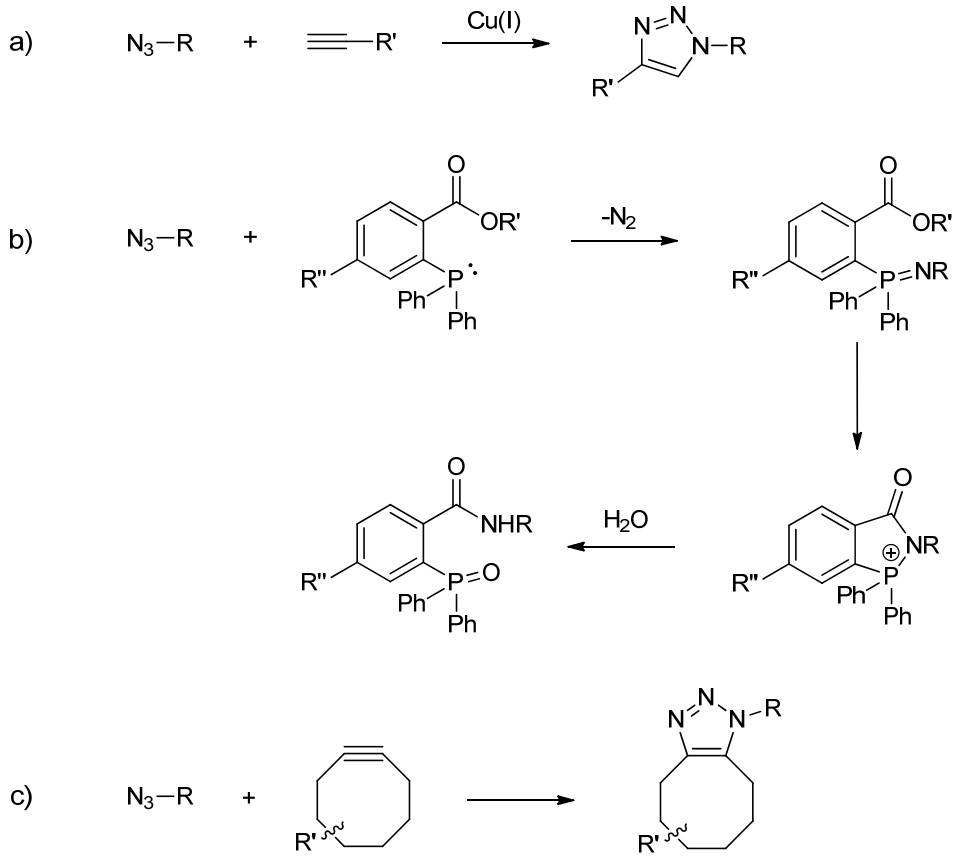

Scheme 1.1. Copper catalyzed cycloaddition reaction between an azide and a terminal alkyne (a), modified Staudinger ligation of an azide with a phosphine (b), and the strain-promoted cycloaddition of an azide with a cyclooctyne (c).

1.4 Objective of This Work

The goal of this thesis is to demonstrate a new *in vivo* targeted drug delivery approach that exploits a click chemistry reaction to selectively bind functionalized NPs to metabolically labeled cancer cells. The overall approach is shown in Figure 1.5. In the first step, azidosugars conjugated to a cancer cell-specific targeting ligand (*e.g.*, an aptamer or antibody that selectively binds to antigens on the surfaces of the cancer cells) will be used to deliver the azidosugars to the targeted cancer cells. Metabolism of the azidosugar results in its incorporation into the glycans that are abundant on the surface of the cancer cells.[28] After metabolically labeling the cancer cells, but not healthy cells, with the azidosugars, NPs that are functionalized with BCN are injected *in vivo*. The click reaction between the azide groups in the membranes of the cancer cells and the BCN moieties on the NPs' surfaces are envisioned to cause the NPs to bind to the cancer cells, and then enter the cells through endocytosis. This approach is expected to avoid the unfavorable biodistribution that occurs in prior active targeting approaches for the following reasons. First, we hypothesize that NPs functionalized with cycloalkynes, such as BCN, do NOT raise any immunogenic issues as compared to NP-antibody or NP-aptamer conjugates because the BCN-functionalized NPs (BCN-NPs) do not contain foreign proteins or DNA fragments. In addition, more proteins bind to the surfaces of NPs functionalized with aptamer or antibody targeting ligands than to unmodified NPs, which can lead to their clearance by the mononuclear phagocyte system (MPS).[7] In contrast, BCN is an organic molecule that is believed to have lower protein binding affinity than other cycloalkyne molecules,[27] which may result in lower protein adsorption and longer circulation times. Overall, this combination of lower accumulation in the liver, spleen and kidneys combined with the enhanced uptake by endocytosis will result in a higher fraction of NPs accumulated in the tumor.

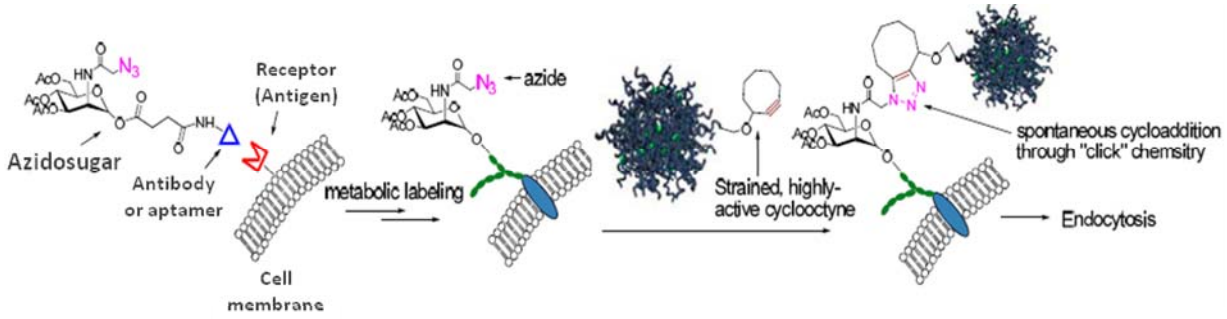

Figure 1.5. Targeted metabolic labeling of cancer cells followed by in vivo "click chemistry" for cancer targeting and therapy.

Along the general goal explained above, Chapter 2 describes our progress in metabolically labeling cells with azidosugars, imaging labeled cells via click chemistry, and binding of BCN modified NPs to the labeled cells. The results show that HeLa and Chinese hamster ovary (CHO) cells can be metabolically labeled with azidosugars and imaged after a click reaction between the azide groups and BCN. In addition, we also demonstrated that fluorescent silica NPs that were functionalized with BCN selectively bound to the cells labeled with azidosugars, whereas no binding was observed on unlabeled cells.

Chapter 3 describes a simple approach to investigate if protein corona affects the targeting yield of functionalized NPs. NPs functionalized with BCN become immobilized on substrates that are modified with azide group due to the click reaction between BCN and the azides. Protein-coated functionalized NPs and protein-free (pristine) functionalized NPs were incubated with the azide-modified wafers, and NP immobilization was assessed. Fluorescence microscopy and scanning electron microscopy (SEM) showed a high number of the pristine NPs were conjugated to the azide-modified substrates whereas few protein-coated NPs were attached to the substrates. These findings confirmed the hypothesis that the protein corona establishes a barrier that inhibits the interactions between the ligand and its target on a separate surface, and significantly reduces NP targeting efficiency. Finally, Chapter 4 explains conclusions and future directions.

CHAPTER 2. TOWARDS THE DEVELOPMENT OF CLICK CHEMISTRY-MEDIATED NANOMEDICINE FOR CANCER CELL TARGETING

Notes and Acknowledgements

This chapter describes unpublished work. Portions of this work were supported by a Career Award at the Scientific Interface from the Burroughs Wellcome Fund (to M. L. Kraft) and NIH 1R21CA152627 (to J. Cheng). V. Mirshafiee was funded by the NIH National Cancer Institute Alliance for Nanotechnology in Cancer Midwest Cancer Nanotechnology Training Center (M-CNTC) Grant. Li Tang assisted with NP synthesis, and Kaiyan Lou assisted with the syntheses of the click chemistry reagents.

2.1 Introduction

Here, we report our progress towards using click chemistry to direct the delivery of fluorescent silica nanoparticles to target cells. In this work, we focus on the click chemistry reaction between an azidosugar (Ac_4GalNAz) and the strained cycloalkyne moiety, bicyclononyne (BCN). As discussed in the Chapter 1, this reaction was selected because it spontaneously occurs under physiological conditions in the absence of toxic copper reagents, and the synthesis of BCN is shorter than that of other reported strained cycloalkynes.[27] We first confirmed the feasibility of using click chemistry for labeling live cells. After synthesis of azidosugar (Ac_4GalNAz) and cycloalkyne (BCN), HeLa and Chinese hamster ovary (CHO) cells were cultured in the presence of azidosugar and incubated with fluorophore-cycloalkyne conjugate (RITC-BCN) to assess whether the cells were labeled through click chemistry. Next, we evaluated whether a click chemistry reaction could be used to label target cells with functionalized NPs. Fluorescent silica NPs were synthesized and functionalized with BCN. Then, CHO cells were metabolically labeled with the azidosugar, fixed, and incubated with functionalized NPs. Finally, the fixed cells were imaged with fluorescent microscope to evaluate NPs binding to the cells.

2.2 Materials and Methods

All the chemicals were purchased form Sigma-Aldrich unless otherwise noted. Bicyclononyne (BCN) **1** was synthesized as shown in Scheme 2.1 following previously reported

procedures.[27] Ac_4GalNAz **2** was synthesized as previously reported (Scheme 2.1).[28] 16% paraformaldehyde solution was purchased from Electron Microscopy Sciences. Fluorescent microscopy images were acquired using a Leica CTR 6000 and a Carl Zeiss LSM 700 confocal microscope.

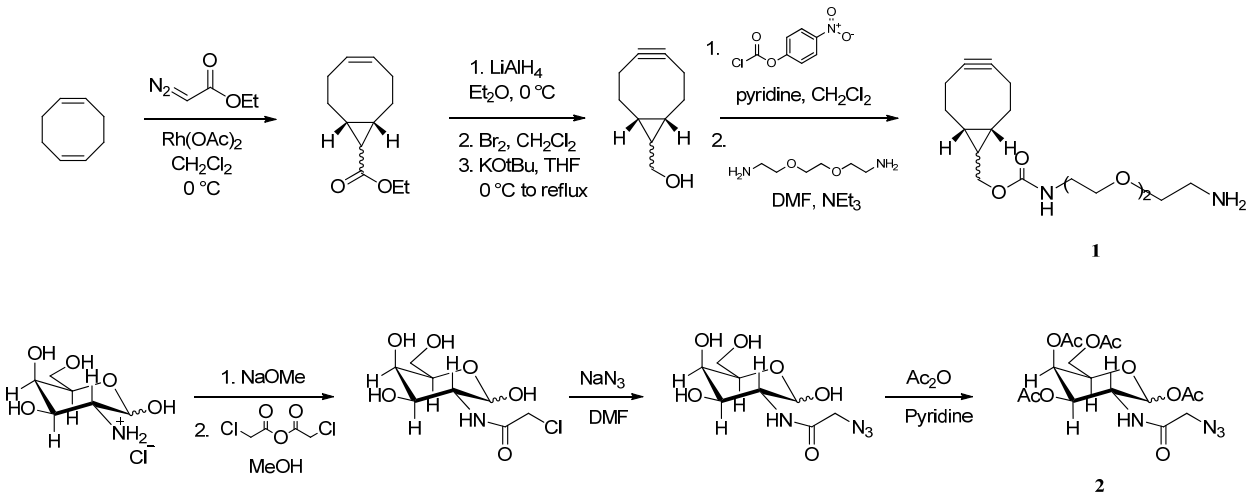

Scheme 2.1. Synthesis of bicyclononyne (BCN) and azidosugar (Ac_4GalNAz).

2.2.1 Synthesis of Rhodamine B isothiocyanate-bicyclononyne conjugate (RITC-BCN, 3)

To a solution of BCN (3 mg, 0.009 mmol) in dimethylformamide (DMF) (1 mL) was added Rhodamine B isothiocyanate (5 mg, 0.01 mmol) and triethylamine (0.01 mL) and the reaction mixture was stirred overnight at rt (Scheme 2.2). The reaction mixture was then concentrated in vacuum and the product was used without further purification.

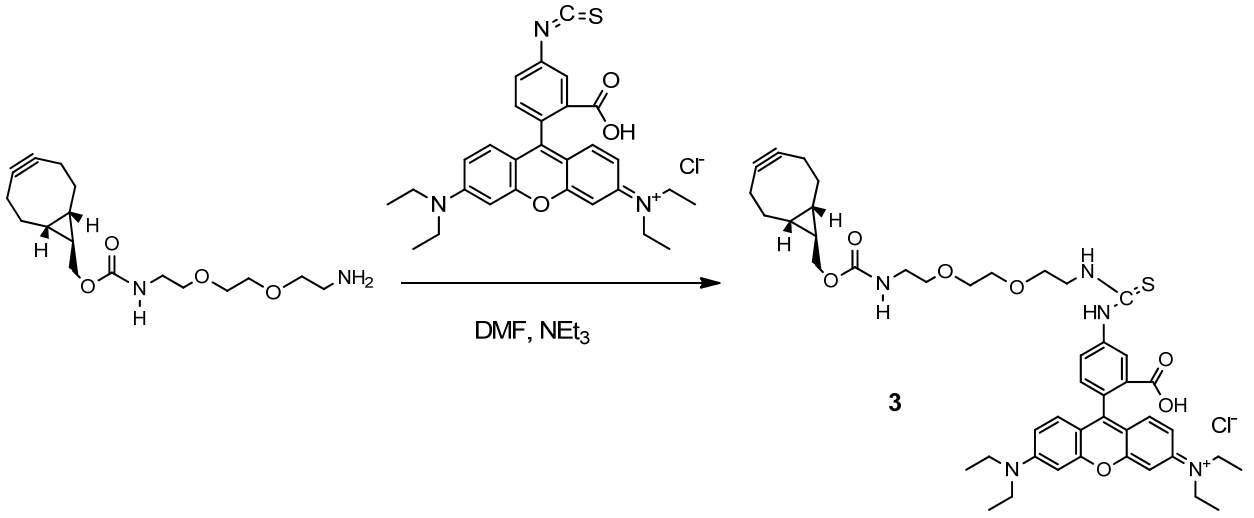

Scheme 2.2. Synthesis of RITC-BCN conjugate.

2.2.2 Synthesis of fluorescent silica NPs

Fluorescent silica NPs were prepared as previously reported.[29] Briefly, 3-aminopropyltrimethoxysilane (30 mg, 0.173 mmol) was added to Rhodamine B isothiocyanate (RITC) (17 mg, 0.032 mmol) in 1 mL ethanol with triethylamine (20 μL, 0.144 mmol). The reaction was stirred for 12 h at 50 °C in the dark. The solvent was evaporated under vacuum, and the crude RITC-silane was dissolved in methanol (10 mg/mL) and used without further purification. Tetraethyl orthosilicate (TEOS) (62.5 μL) was added to a mixture of methanol (1 mL), deionized (DI) water (0.36 mL) and concentrated ammonia (0.08 mL). The mixture was stirred at 150 rpm for 2 h, RITC-silane solution (25 μL of 10 mg/mL methanol) was added to the mixture, and the solution was stirred at 150 rpm at rt for 12 h. To functionalize the resulting silica NPs with amine moieties, 3-aminopropyltrimethoxysilane (3 μL) and TEOS (1 μL) were added to the NP solution and the reaction was stirred for 12 h. NPs were collected by centrifugation and washed with ethanol three times.

2.2.3 Synthesis of BCN-functionalized silica NPs (BCN-NPs)

Scheme 2.3 summarizes the conjugation of BCN to the surface of the NPs. Silica NPs (11 mg) were dispersed in a 10% solution of succinic anhydride in DMF, and stirred overnight at rt. The NPs were collected by centrifugation, and washed three times with DMF. The resulting carboxylic acid-functionalized NPs (2 mg) were dispersed in 2-(N-morpholino)ethanesulfonic acid (MES) buffer (1.5 mL, 0.1 M, pH 6.8), and 1-ethyl-3-(3-dimethylaminopropyl) carbodiimide (50 mg, 0.261 mmol) and *N*-hydroxysuccinimide (50 mg, 0.434 mmol) were added to the solution. The mixture was stirred for 25 min at rt. The NPs were collected by centrifugation, washed with DI water, and then dispersed in phosphate buffered saline (PBS) (1 mL, pH 7.4). BCN (5 mg) in methanol (50 μL) was added to NP solution and the reaction was stirred overnight. The resulting BCN-NPs were collected by centrifugation, washed three times with methanol, and suspended in deionized (DI) water.[30]

2.2.4 Cell culture

HeLa and CHO (Chinese hamster ovary) cells were grown in eagle's minimal essential medium (DMEM) or Ham F12 media supplemented with 10% fetal bovine serum (FBS) and 1% penicillin/streptomycin in a 5% CO_2 incubator at 37°C.

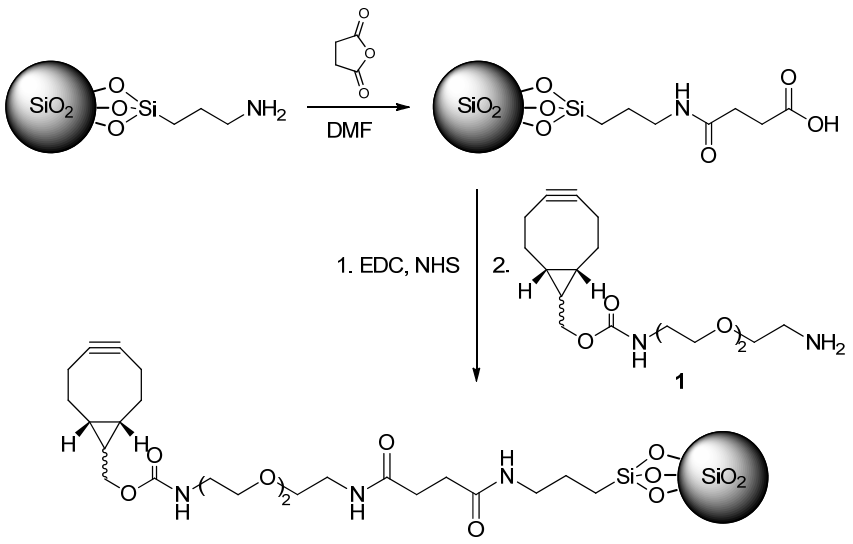

Scheme 2.3. Surface modification of silica NPs with BCN.

2.2.5 Live cell labeling and imaging

HeLa cells were seeded at a density of 20,000 cells per well in 1 mL DMEM with 10% FBS (HyClone Laboratories) on 4-well Nunc Lab-Tek Chambered Cover Glass microscopy slides (Fisher). Cells were incubated with 50 μM of Ac_4GalNAz for 40 h at 37 °C. HeLa cells incubated without Ac_4GalNAz served as negative controls. The cells were rinsed with media three times and each well was filled with 50 μM BCN-RITC (diluted from a 10 mM dimethyl sulfoxide **(**DMSO) stock solution) in media and incubated for 15 min at 37 °C. The cells were rinsed with PBS and imaged with a fluorescence microscope at ambient temperature.

CHO cells were cultured at a density of 10,000 cells in 2 mL media on 35 mm plastic dish (Sarstedt). Cells were grown with Ac_4GalNAz at 50 μM concentration for 3 days at 37 °C. The cells were rinsed with FACS buffer (PBS containing1% FBS) for three times and each well was filled with 5 μM BCN-RITC in FACS buffer and incubated for 5 min at 37 °C. Cells were washed with FACS buffer for four times and imaged under confocal microscope.[31]

2.2.6 Labeling fixed CHO cells with fluorescent NPs

CHO cells were cultured with Ac_4GalNAz as described above. After three days, the media was removed and cells were washed with PBS and fixed with 4% paraformaldehyde (dilution of 16% solution in PBS). The fixed cells were incubated with 100 μg of functionalized NPs (BCN-

NPs) in PBS (1 mL) for 1 h, and then were washed with PBS five times. After that, the cells were imaged with fluorescence microscope.

2.3 Results and Discussion

First, we evaluated the feasibility of labeling live cells and imaging them with click chemistry. HeLa and CHO cells were grown in the presence of Ac_4GalNAz (50 μM) in order to metabolically incorporate the azidosugar into the glycans on the cell surface (experimental cells). HeLa and CHO cells that were grown in the absence of Ac_4GalNAz were used as a negative control. Next, the experimental and negative control cells were treated with RITC-BCN. As shown in Figure 2.1.a and c, azidosugar-treated cells exhibited high fluorescence, which demonstrates the click chemistry reaction occurred between the metabolically incorporated cell surface azides and RITC-BCN. In comparison, the negative control cells exhibited significantly weaker fluorescence, likely caused by the non-specific adsorption of RITC-BCN to the cells' surfaces (Figure 2.1.b and d).

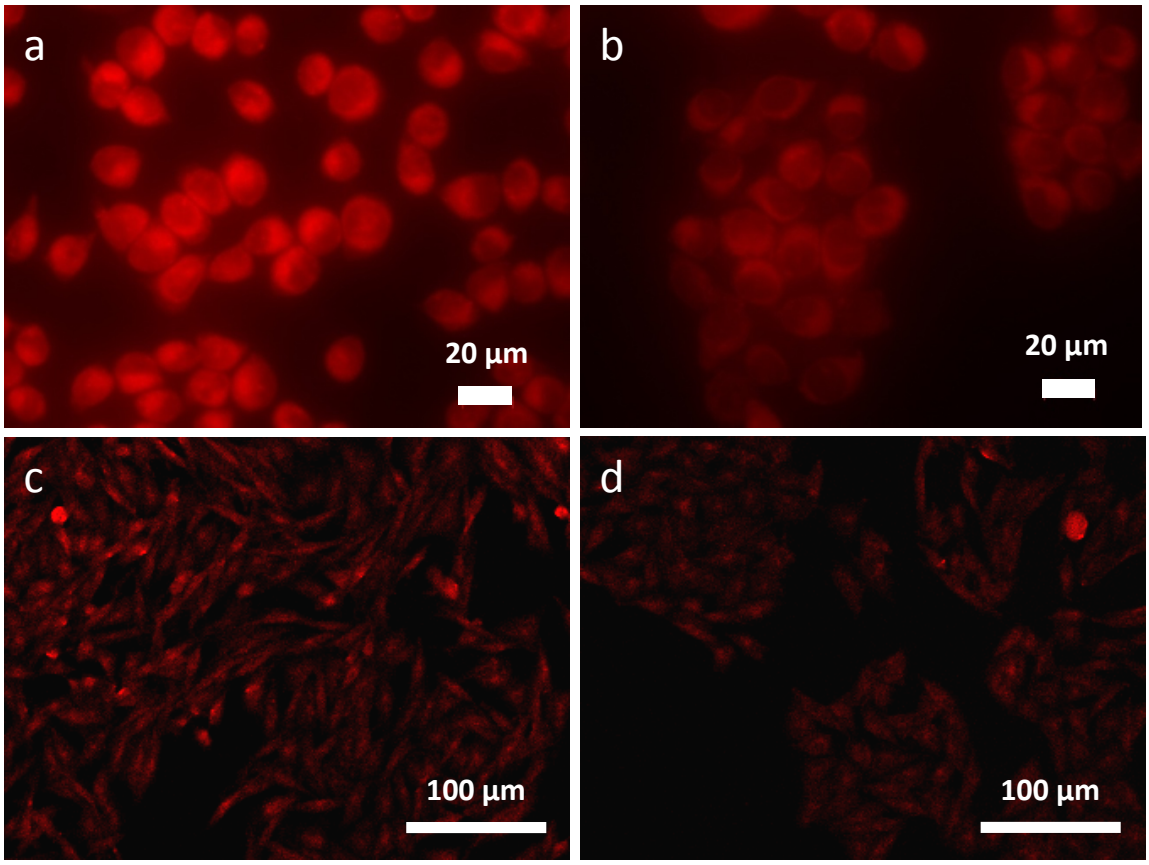

Figure 2.1. Fluorescence microscopy images of HeLa and CHO cells after incubation with RITC-BCN. (a and c) HeLa and CHO cells that were metabolically labeled with Ac_4GalNAz exhibited strong fluorescence that indicated the RITC-BCN undergone a click chemistry reaction with the azides on the cell surface. (b and d) HeLa and CHO cells grown in the absence of Ac_4GalNAz exhibited much weaker fluorescence that was likely caused by nonspecific adsorption of the dye to their surfaces.

Having confirmed that metabolically incorporated cell surface azides were accessible for a click chemistry reaction, we next evaluated whether the click reaction targeted fluorescent silica NPs that were functionalized with BCN to bind to cells with metabolically incorporated azidosugars on their surfaces. CHO cells were metabolically labeled with Ac_4GalNAz and fixed prior to incubation with the functionalized NPs. Fixation was used to exclude the possibility that the NPs were nonspecifically uptaken by the cells, thereby ensuring that only NP binding to the cells would be detected by fluorescence microscopy. The fluorescence microscopy images show

that NPs bound to the surfaces of the cells that were metabolically labeled with the azidosugars, but not to the cells that were not metabolically labeled with azidosugars (Figure 2.2).

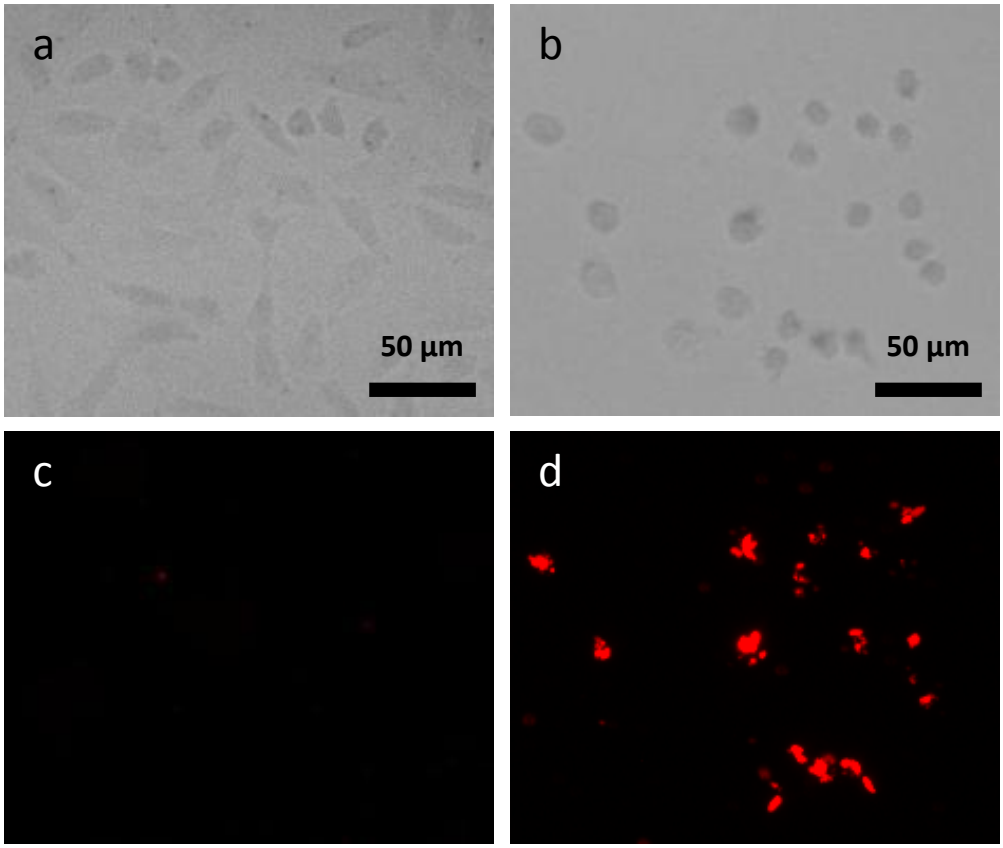

Figure 2.2. Bright field and fluorescence microscopy images of CHO cells treated with BCN-NPs. (a and c) CHO cells cultured in the absence of $Ac_4GalNAz$ were not labeled with BCN-functionalized NPs. (b and d) The high fluorescence intensity indicates the CHO cells that were metabolically labeled with $Ac_4GalNAz$ had BCN-functionalized NPs conjugated to their surfaces**.**

These results confirm that the click chemistry reaction between the BCN on the NPs and the azidosugars on the cells' surfaces can be used to selectively label target cells with NPs. Although metabolic labeling can be achieved *in vitro* by adding the azidosugar to the cell culture medium, subsequent work must be completed to enable the selective delivery of the azidosugar, and thus, metabolic labeling, of the target cancer cells *in vivo*. Promising approaches for achieving this goal are discussed in the Chapter 4.

CHAPTER 3. PROTEIN CORONA SIGNIFICANTLY REDUCES ACTIVE TARGETING YIELD

Notes and Acknowledgements

This chapter was co-authored by Vahid Mirshafiee, Morteza Mahmoudi, Kaiyan Lou, Jianjuan Cheng, and Mary L. Kraft. It has been published in Chemical Communications (DOI: 10.1039/C3CC37307J),[32] and is reproduced by permission of The Royal Society of Chemistry. Portions of this work were carried out in the Metabolomics Center in the Roy J. Carver Biotechnology Center, Univ. of Ill., and the Frederick Seitz Materials Research Laboratory Central Facilities, Univ. of Ill., which is partially supported by the U.S. Department of Energy (DOE) under grants DEFG02-07ER46453 and DE-FG02-07ER46471. Portions of this work were supported by a Career Award at the Scientific Interface from the Burroughs Wellcome Fund (to MLK) and NIH 1R21CA152627 (to JC). VM was funded by the NIH National Cancer Institute Alliance for Nanotechnology in Cancer Midwest Cancer Nanotechnology Training Center (M-CNTC) Grant. The authors thank Li Tang for assistance with NP synthesis and Qian Yin for zeta potential measurements.

3.1 Introduction

NPs are promising materials for the targeted delivery of therapeutic drugs to the desired site in the human body.[8] One strategy to obtain a high targeting yield is to functionalize the surface of the NPs with targeting ligands (*e.g.* antibodies or aptamers) that enhance NP binding to receptors on the target cells and facilitate NP uptake by receptor-mediated endocytosis.[33,34] *In vitro* results generally confirm the high capability of functionalized NPs for targeting to the desired cells. However, lower targeting yields and an unfavorable biodistribution (i.e., NP accumulation in the liver and spleen instead of the desired tumor tissue) is often observed *in vivo*.[6]

The discrepancy between the *in vitro* and *in vivo* results is due, in part, to the adsorption of proteins and other biomolecules to the NP's surface upon exposure to the biological medium *in vivo*.[8-10] In contrast, the NP surface remains nearly pristine in the presence of the serum-free medium that is often used for *in vitro* studies of NP uptake.[8] Therefore, cells in *in vitro* experiments that employ serum-free medium interact with the original NP surface, whereas cells

in vivo interact with the protein coating, which is called the protein corona.[8-10] The presence of the protein corona on the NP, which is strongly related to the physicochemical properties of the NP and protein sources,[7,35,36] is reported to alter the biodistribution, cellular uptake mechanism, and intracellular location of the NPs *in vivo*.[6,12,37-39] In addition to these changes in biological phenomena, the protein corona may compromise the targeting efficiency of NPs that are functionalized with targeting ligands via a non-biological mechanism. Specifically, the protein corona surrounding the NP is hypothesized to hinder interactions between the NP's ligands and their targets on the cell surface,[6] though this mechanism has not been directly tested. Thus, the main aim of this work is to investigate whether the protein corona inhibits NP ligand binding to reactive moieties on a surface.

To permit separating the protein corona's effects on biological phenomena (i.e., uptake mechanism) from its potential ability to limit access to the targeting ligand, we selected a copper-free click reaction between NPs functionalized with a strained cycloalkyne, BCN, and an azide on a silicon substrate as the model targeting reaction (Scheme 3.1).

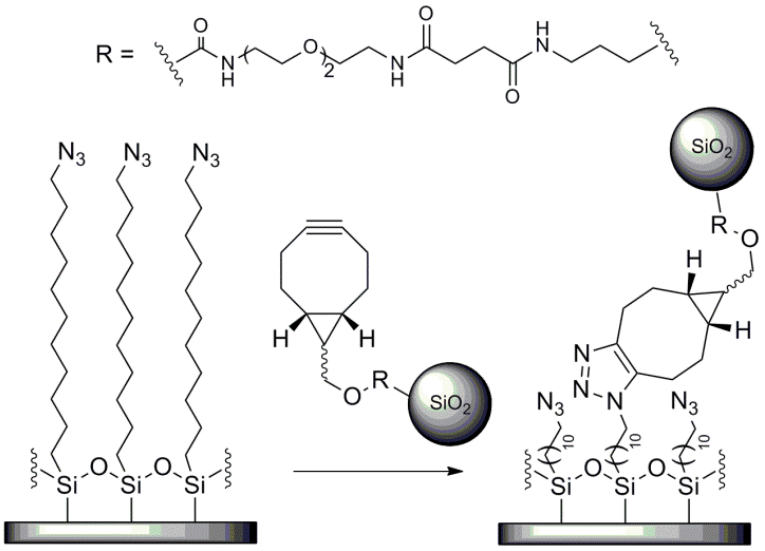

Scheme 3.1. A copper-free click reaction between the BCN moieties on the NPs and the azides on the modified silicon substrate was selected as the model targeting reaction.

We prepared fluorescent silica NPs with diameters of 75 nm using the Stöber method[29] and then conjugated BCN targeting ligands to the NP surface. Silicon substrates were modified with an azide-terminated self-assembled monolayer (SAM). We evaluated whether BCN-NP conjugation to the azide-functionalized substrates was reduced by the protein corona that results

from exposing the BCN-functionalized silica NPs (BCN-NPs) to biological fluids. We compared the conjugation of pristine BCN-NPs to those of BCN-NPs exposed to mediums that mimic *in vitro* culture conditions (i.e., medium with 10% serum) and the biological fluids present *in vivo* (i.e., 100% serum). Pristine BCN-NPs and BCN-NPs exposed to medium with 10% serum (10% serum corona BCN-NPs) or 100% serum (100% serum corona BCN-NPs) were incubated with azide-functionalized substrates, and then conjugation was assessed with fluorescence microscopy and SEM.

Finally, liquid chromatography-mass spectrometry/mass spectrometry approach (LC-MS/MS) was used to assess the compositions of the protein coronas on the BCN-NPs that resulted from exposure to mediums that mimic the *in vitro* (10% serum) or *in vivo* (100% serum) environments.

3.2 Materials and Methods

All the chemicals were purchased form Sigma-Aldrich unless otherwise noted. Silicon substrates (5 mm by 5 mm diced silicon wafers) were purchased from Ted Pella, Inc. PBS was purchased from Lonza. FBS was purchased from HyClone Laboratories. BCN **1** was synthesized as shown in Scheme 2.1 following previously reported procedures.[27] 11-Azidoundecyltrimethoxysilane **3** was synthesized from 11-bromoundecyltrimethoxysilane (GelSet, Inc.) as previously reported.[40] Sequencing Grade Trypsin was purchased from G-Biosciences (St. Louis, MO). Fluorescent microscopy images were acquired using a Leica CTR 6000. SEM images were acquired on a Hitachi S4800 high resolution SEM. X-ray photoelectron spectrometry (XPS) spectra were acquired on a Physical Electronics PHI 5400. Size measurements were acquired using a ZetaPlus dynamic light-scattering (DLS) detector (Brookhaven Instruments). Zeta potential was measured with a Malvern Zetasizer 3000 (Malvern Instruments). BCN-functionalized NPs were synthesized as it was reported in chapter 2.

3.2.1 Modification of silicon substrates with an azide-terminated self-assembled monolayer (SAM)

Silicon substrates (5 mm by 5 mm) were cleaned in a freshly prepared piranha solution (H_2SO_4/H_2O_2, 4:1) for 30 min. (*Extreme caution must be used when cleaning with piranha solution. Gloves, goggles, and face shield should be used for protection.*) The substrates were

thoroughly rinsed in deionized (DI) water and air dried. To functionalize the substrate with an azide-terminated SAM, the silicon substrates were immersed in a 70 °C solution of 11-azidoundecyltrimethoxysilane in toluene (1:9 v/v) with a trace amount of water (1 drop) for 2 h with occasional stirring (Scheme 3.2).[41] After cooling to rt, the substrates were sonicated in fresh toluene for 5 min, washed with acetone, dichloromethane, methanol and DI water, and air dried.[42] XPS analysis of the substrates confirmed the presence of the terminal azides on the SAM (Figure 3.1).

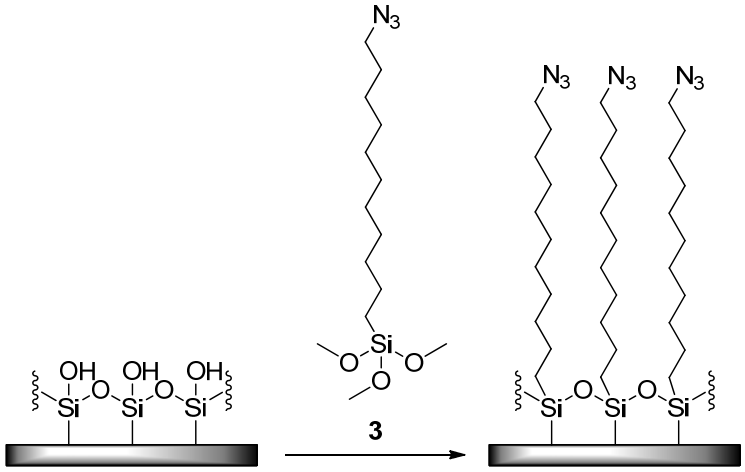

Scheme 3.2. Modification of silicon substratewith an azide-terminated SAM.

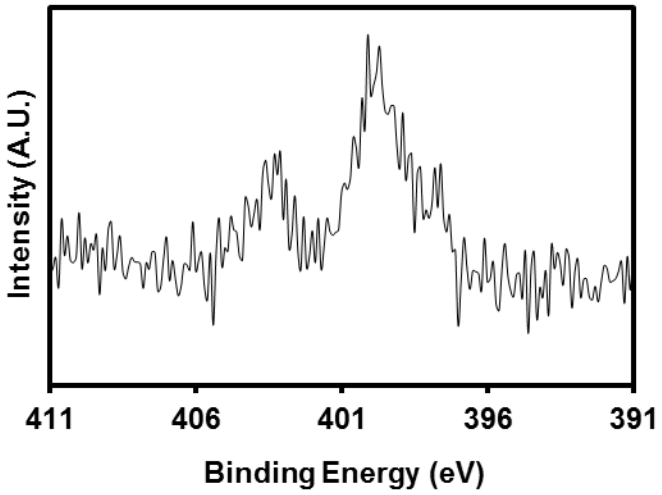

Figure 3.1. XPS data of SAM-modified silicon substrates confirms the presence of terminal azides. The photoelectron spectra of the nitrogen 1s binding energies shows the two peaks at 400 and 404 eV that are characteristic of azides.[43]

3.2.2 Preparation of hard corona NPs

The adsorption of serum proteins to the BCN-NPs was probed by exposing the NPs to mediums containing 10% or 100% FBS. An aqueous solution of BCN-NPs (100 μL, 2 mg/mL in DI water) was mixed with 900 μL of FBS solution (10% FBS in PBS, or 100% FBS, respectively), and the solution was incubated at 37°C for 1 h. This incubation time was selected because it is reported to produce a protein corona with a relatively stable composition, and little change in composition occurs after 1 h.[10] Each sample of BCN-NPs in the FBS solution was centrifuged at 10,000g for 30 min, the supernatant was carefully removed, and the protein-coated BCN-NPs were suspended in 500 μL of PBS. To ensure the excess (unbound or loosely bound) proteins were removed from the BCN-NP solution, which is critical for subsequent analysis of the protein composition of the hard corona on the BCN-NPs, the centrifugation process was repeated three times, and then the BCN-NPs were dispersed in cold PBS.

3.2.3 Size and zeta potential analysis.

Measurements were made on pristine, 10% serum corona, and 100% serum corona BCN-NPs that were dispersed in PBS at a concentration of 100 μg/mL. The results are summarized in Table 3.1.

	Pristine	10% serum corona	100% serum corona
size (d, nm)	154	383	634
polydispersity index	0.19	0.28	0.34
zeta potential (mV)	-18.9	-16.6	-7.9

Table 3.1. Size (hydrodynamic diameter, d), size distribution (polydispersity index, PDI), and zeta potential of BCN-NPs in PBS, determined by DLS.

3.2.4 Conjugation of BCN-NPs to silicon substrates

For each type of BCN-NP (pristine BCN-NPs, 10% serum corona BCN-NPs, and 100% serum corona BCN-NPs), a NP solution (200 μg of NPs in 500 μL of PBS) was added to an azide-modified silicon substrate and incubated for 90 min at rt while stirring at 300 rpm. Non-

specific BCN-NP binding was assessed by incubating a solution of pristine BCN-NPs (200 μg in 500 μL PBS) in the presence of a substrate that was not functionalized with azides for 90 min at rt while stirring at 300 rpm. For all samples, the unconjugated NPs were removed by rinsing in DI water. Then the samples were dried in ambient air, and conjugation was assessed by imaging with fluorescence microscopy and SEM.

3.2.5 Statistical analysis of reduction in targeting efficiency

The reduction in targeting efficiency due to protein adsorption was quantified by comparing the average numbers of (i) pristine BCN-NPs, (ii) 10% serum corona BCN-NPs, and (iii) 100% serum corona BCN-NPs on the 5 x 5 mm azide-functionalized substrates. As a negative control, the number of pristine BCN-NPs on the 5 x 5 mm azide-free substrates was also assessed. Using Image J, a threshold fluorescence intensity level that represented NPs within the mosaic of images of the substrate was set, and the number of pixels that exceeded this threshold was counted. For each experimental condition, two 5 x 5 mm substrates were analyzed, and the average number of BCN-NPs was calculated. The conjugation efficiency of the BCN-NPs exposed to serum-containing medium was calculated by dividing the average number of 10 or 100% serum corona BCN-NPs on the substrate by the average number of pristine BCN-NPs per substrate and multiplying the resulting fraction by 100. The conjugation efficiency of the 10% and 100% serum corona BCN-NPs were 5% and 1%, respectively, that of the pristine BCN-NPs. Therefore, the targeting efficiency for the 10% and 100% serum corona BCN-NPs was 94 and 99%, respectively, lower than that of the pristine BCN-NPs.

3.2.6 Composition analysis of protein coronas on BCN-NPs with liquid chromatography-mass spectrometry/mass spectrometry (LC-MS/MS)

The BCN-NPs exposed to mediums containing 10% or 100% FBS were collected by centrifugation at 20,000g for 10 min, and the pellet was resuspended in 25 of Sequencing Grade Trypsin (25 μL, 12.5 ng/μL in 25 mM ammonium bicarbonate), and digested using a CEM Discover Microwave Digestor (Mathews, NC) for 15 min at 55 °C (70W). Digestion was stopped by the addition of 200 μL of an acetonitrile/water/formic acid (50:45:5 v/v/v) solution. The solvents were removed using a Thermo SpeedVac, and the residue was dissolved in 13 μL of aqueous acetonitrile (5% acetonitrile) containing 0.1% formic acid. Samples (10 μL) were

analyzed by LC-MS/MS performed on a Waters quadrupole time-of-flight mass spectrometer (Q-ToF) connected to a Waters nanoAcquity UPLC. LC was performed on a Waters Atlantis C-18 column (0.03 mm particle, 0.075 mm x 150 mm) using a flow rate of 250 nL/min. Peptides were eluted using a linear gradient of aqueous acetonitrile (0-60% acetonitrile) containing 0.1% formic acid in 240 min. The mass spectrometer was set for data dependent acquisition, and MS/MS was performed on the most abundant four peaks detected at any given time. Data were analyzed using the Waters Protein Lynx Global Server 2.2.5, Mascot (Matrix Sciences) and Blasted against NCBI NR database specific for Bostaurus. The normalized percentage of spectral counts detected by LC-MS/MS for protein k (NpSpCk) was calculated according to Equation 1.[9]

$$\mathrm{NpSp\,C_k} = \left(\frac{\left({}^{\mathrm{SpC}}/_{(\mathrm{M_w})_k} \right)}{\sum_{i=1}^{n} \left({}^{\mathrm{SpC}}/_{(\mathrm{M_w})_i} \right)} \right) \times 100 \qquad (1)$$

3.3 Results and Discussion

The fluorescence microscopy images of substrates incubated with pristine and protein coated BCN-NPs are shown in Figure 3.2. Experiments in which pristine BCN-NPs were incubated with azide-free substrates confirmed that non-specific BCN-NP binding to the substrate was insignificant (Figure 3.2a). The fluorescence microscopy images show a high number of the pristine BCN-NPs were conjugated to the azide-functionalized substrate (Figure 3.2b). In contrast, fluorescence microscopy showed few 10% or 100% serum corona BCN-NPs had attached to the azide-functionalized substrates (Figure 3.2c and d). Quantitative analysis indicated that the number of conjugated NPs, and therefore the targeting efficiencies for the 10% and 100% serum corona BCN-NPs were lower than that of the pristine BCN-NPs by 94 and 99%, respectively. SEM imaging confirmed these fluorescence microscopy results. The SEM images show numerous pristine BCN-NPs, but very few 10% or 100% serum corona BCN-NPs conjugated to the azide-functionalized substrates (Figures 3.3). These findings indicate the protein corona inhibits the NP's targeting capability.

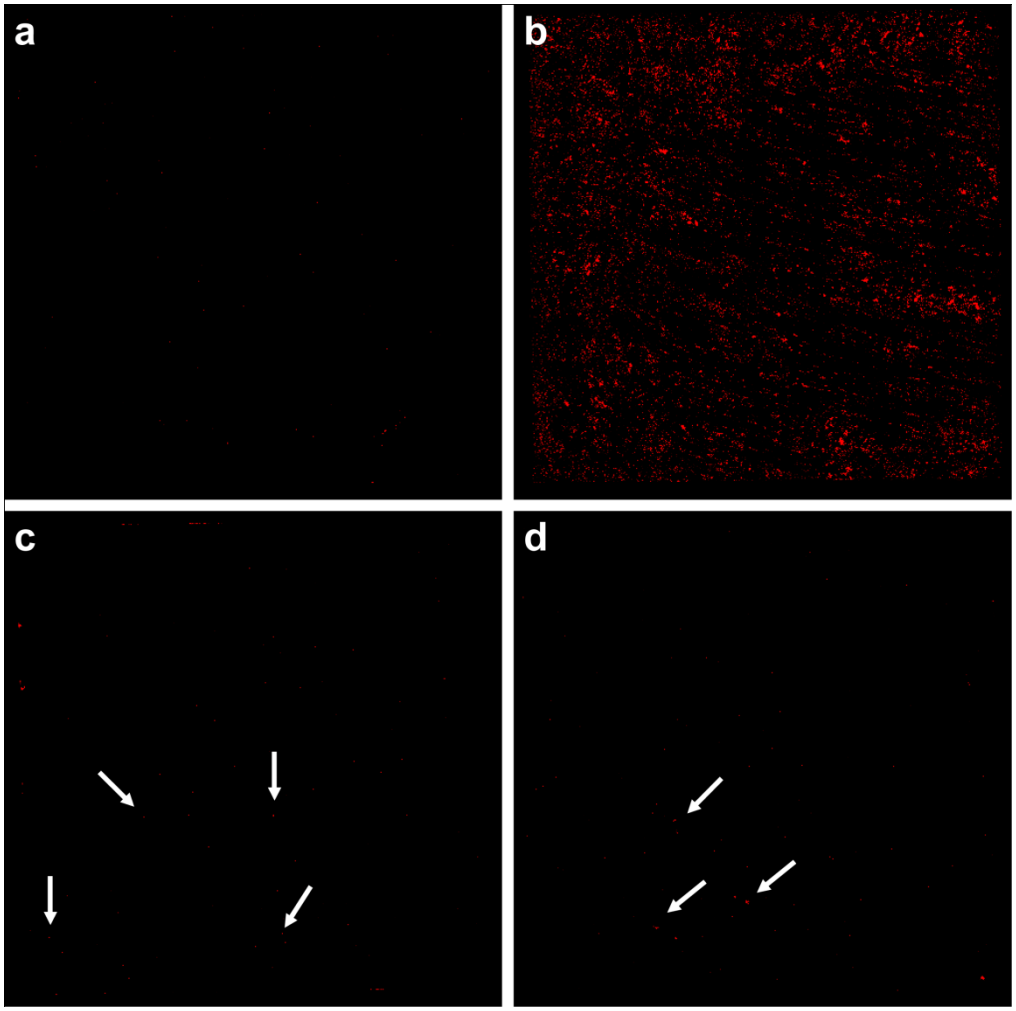

Figure 3.2. Fluorescence microscopy images of 5 mm by 5 mm silicon substrates after incubation with pristine BCN-NPs and those coated with a protein corona. (a) Little non-specific binding of pristine BCN-NPs to the azide-free substrate occurred. (b) Numerous pristine BCN-NPs were conjugated to the azide-functionalized substrate. (c and d) Few10% (c) or 100% (d) corona BCN-NPs were visible on the azide-functionalized substrates. Arrows designate individual NPs.

Characterization of the BCN-NPs in terms of size and zeta potential indicated that exposing the BCN-NPs to medium containing 10% or 100% serum increased their size, but only slightly decreased their negative charge (Table 3.1). The increase in size upon exposure to serum-containing media reflects formation of the protein corona as well as larger protein-NP complexes.[44] The slight decrease in negative charge is due to screening of the negatively charged surface of the silica NP by the protein corona, and should not drastically alter the interactions

between the substrate and the BCN-NPs in these experiments. Although NP uptake by cells is very size-dependent,[7] we do not expect that the approximately two-fold increase in BCN-NP diameter that occurred after exposure to 10% serum medium is the primary cause of the ~94% reduction in targeting efficiency we observed under these conditions. Therefore, the protein corona-induced inhibition of NP targeting capability we observed in this system was mainly caused by screening of the interactions between the NP's targeting ligands and their reactive partners on the substrate.

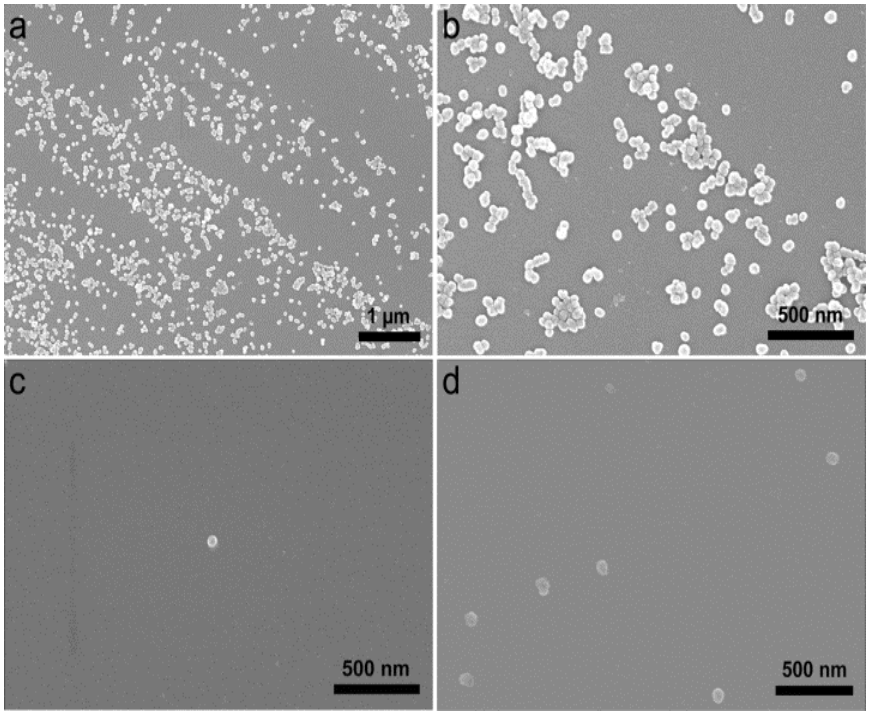

Figure 3.3. SEM images of silicon substrates modified with azide-terminated SAMs after incubation with pristine BCN-functionalized NPs.

The composition of protein corona on the BCN-NPs was assessed using a liquid chromatography-mass spectrometry/mass spectrometry approach (LC-MS/MS). A comprehensive list of the proteins detected in the coronas on the 10% and 100% serum corona BCN-NPs are listed in Table 3.2. Evaluation of the normalized abundances of proteins within a specific molecular weight range (Figure 3.4) indicated that ≥88% of the proteins in the coronas on the BCN-NPs exposed to either serum-containing medium had a molecular weight below 30 kDa. Despite their relatively low molecular weights, these proteins established a shell that significantly reduced the BCN targeting ligand's ability to react with the azides on the surface.

Although Table 3.2 shows that the proportions of the different proteins within each of the two coronas differed, the proportions of proteins with a specific molecular weight range, and the reduction in NP conjugation were very similar. Thus, the protein's molecular weight is the main factor correlating its propensity to adsorb to the NP and obstruct its targeting ligands.

Molecular Weight (Da)	Protein Name	NpSpC	
		10% serum corona	100% serum corona
451,342	dynein, axonemal, heavy chain 5	0.03	0
248,286	factor V	0.32	0
91,157	plasminogen precursor	0.19	0
90,229	BR serine/threonine kinase	0	0.13
85,836	integrin beta-6 precursor	0	0.19
71,659	E3 SUMO-protein ligase PIAS1	0	0.18
68,543	alpha-fetoprotein precursor	0.31	0.41
66,088	serum albumin	0.41	1.12
53,541	vitronectin	0.30	0
48,427	kininogen I precursor	0.28	0
48,118	kininogen II precursor	0	0.62
46,075	alpha-1-antiproteinase precursor	0.98	1.73
35,847	apolipoprotein E	2.41	0
30,253	apolipoprotein A-I precursor	6.05	5.96
15,849	hemoglobin fetal subunit beta	18.54	12.34
15,044	Chain A, A Novel Allosteric Mechanism In Haemoglobin	32.25	47.28
12,544	60S ribosomal protein L35a	0.89	0
11,195	apolipoprotein A-II precursor	16.27	10.19
2,337	fetuin	20.74	19.91

Table 3.2. Comprehensive list of normalized percentage of each protein identified by LC-MS/MS in the hard coronas on the BCN-NPs that were incubated for 1 h in medium containing 10% and 100% FBS.

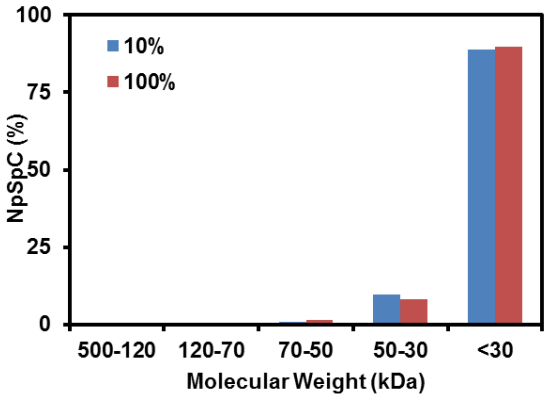

Figure 3.4. Normalized spectral counts (NpSpC) of proteins with the specified range of molecular weights detected in the hard coronas on the BCN-NPs incubated for 1 h in medium containing 10% and 100% FBS.

Altogether, this study confirms the hypothesis that the protein corona establishes a barrier that screens the interactions between the ligand and its target on a separate surface (i.e., the cell membrane), thereby significantly reducing NP targeting efficiency as compared to NPs with pristine surfaces. We found that BCN-NP exposure to medium that contained as little as 10% serum, which is the typical serum concentration used for mammalian cell culture, resulted in the formation of a protein corona that significantly inhibited the model targeting reaction we studied. Our results imply that, in addition to NP clearance from the body (i.e., unfavorable biodistribution), screening of the targeting ligand by the protein corona that forms upon NP exposure to biological fluids contributes to the lower the NP targeting efficiencies attained *in vivo* than *in vitro*. Given that protein absorption to the NP surface cannot be prevented, as even modification of NPs with polyethylene glycol (PEG) reduces, but does not prevent, protein absorption,[45] screening of the NP's targeting ligand due to protein absorption must be considered when designing NPs for targeted drug delivery. Because the click chemistry reaction between BCN-NPs and the azide-functionalized surfaces used in this study enables separating the protein corona's ability to obstruct the targeting ligand from its effects on biological phenomena, this approach may simplify assessing the extent that NPs with various surface modifications are screened by the protein corona. We expect that increased consideration of targeting ligand screening by the protein corona that surrounds the NP will help to improve the efficiency of NP uptake *in vivo*.

CHAPTER 4. CONCLUSIONS AND FUTURE DIRECTIONS

To selectively deliver anti-cancer drugs to tumors, various NPs have been developed and their surface have been functionalized with targeting ligands that can bind to the receptors on the cancer cell membrane. Despite the initial expectation that the targeting ligands on the NPs would significantly increase in *in vivo* targeting efficiency, this approach did not considerably improve NP uptake by cancer cells. Instead, a large fraction of functionalized NPs typically accumulate in the liver and spleen. To address this challenge, we have designed a new targeting approach that involves metabolic cell labeling and click chemistry. In this approach, a saccharide derivative modified with an azide group (azidosugar) is metabolically incorporated into the glycans on the cancer cell membrane. Then, NPs that are functionalized with a reactive cycloalkyne, BCN, would be added to the cells. Through the spontaneous click reaction between the azide groups and bicyclononynes, the NPs would bind to the cancer cell membrane, which leads to their uptake via endocytosis. In this thesis, we demonstrated that HeLa and CHO cells could be metabolically labeled with an azidosugar and imaged by detection of fluorophore -BCN conjugate attached to the cell surface via a click chemistry reaction. In addition, we showed that NPs functionalized with BCN selectively bound to CHO cells that were metabolically labeled with the azidosugar, while there was no binding for cells that had not been metabolically labeled. Altogether, these results suggest that the proposed click chemistry approach will enable targeting NPs to metabolically labeled cells.

To use this approach for *in vivo* targeting, only the cancer cells should have metabolically incorporated azidosugars on their surfaces. Thus, the azidosugars need to be selectively delivered to the cancer cells, but not healthy cells, prior to the administration of BCN-functionalized NPs. The future direction to achieve this aim is to conjugate the azidosugar to a targeting ligand, such as an antibody or aptamer, which selectively binds to the cancer cells. This is expected to increase the conjugate uptake by the cancer cells, and subsequent metabolic incorporation of the azidosugar into the glycans on the cancer cells' surfaces. After the cancer cells are selectively labeled, BCN-functionalized NPs would be administered and their targeting efficiency would be evaluated.

To obtain a desirable targeting efficiency for functionalized NPs, the targeting ligands on the NP's surface must be accessible for interaction with the receptors on the cell membrane.

However, upon exposure to the biological environment, the NPs become covered with proteins and biomolecules. By using a click reaction as the model targeting reaction, we showed that this protein coating, called the protein corona, established a barrier that screened the targeting ligand, BCN, and prevented it from interacting with its azide targets on a silicon substrate (Figure 4.1). These results suggest that in addition to NP clearance from the body, the protein corona also contributes to the low targeting yields obtained in many *in vivo* studies.

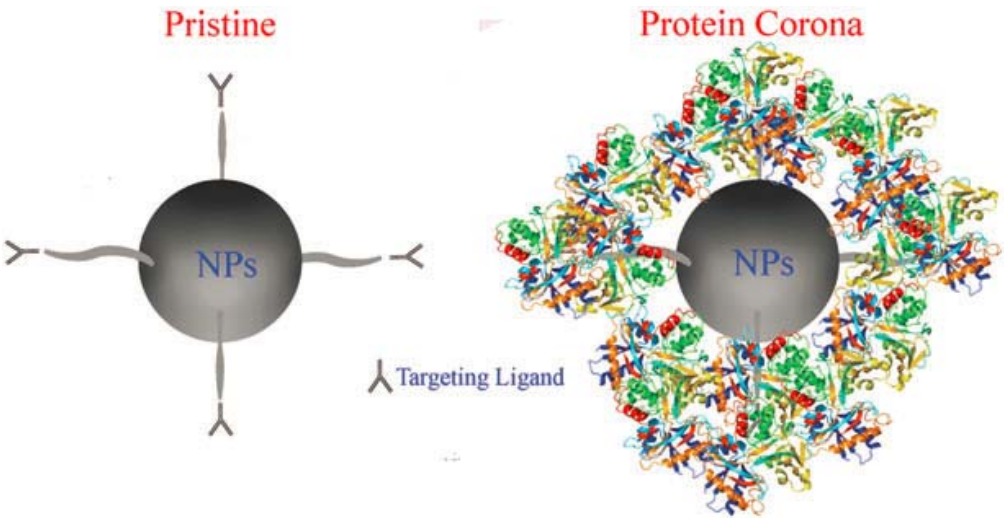

Figure 4.1. Simplified schematic of protein corona-induced screening of NP targeting ligands, which reduces targeted NP delivery. The protein corona covers the targeting ligands on the NP, preventing the ligands from binding to their targets on a separate surface (i.e., a cell).

The click chemistry reaction between BCN-functionalized NPs and azides on a silicon surface provides a simple approach to assess the extent of targeting ligand screening. However, a cell-based platform would be required to assess the changes in biological phenomena that are induced by the protein corona, and how its composition may change as the NPs are trafficked through the endocytic compartments.[46,47] Alternatively, one might exploit the protein corona as a targeting ligand.[6,48] For example, the high vitronectin content in the protein corona of cationic lipid/DNA complexes enhances targeting to MDA-MB- 435S cancer cells, a cell line derived from M14 melanoma cells, that overexpress the two major vitronectin receptors, αβv3 and αβv5 integrins.[48] Overall, we expect that increased consideration of targeting ligand screening by the protein corona that surrounds the NP will help to improve the efficiency of NP uptake *in vivo*.

REFERENCES

1- R. Siegel, D. Naishadham and A. Jemal, *CA Cancer J Clin*., **2012**, 62, 10–29.

2- D. Peer, J. M. Karp, S. Hong, O. C. Farokhzad, R. Margalit and R. Langer, *Nature Nanotech*., **2007**, 2, 751-760.

3- R. A. Petros and J. M. DeSimone, *Nat Rev Drug Discov*, **2010**, 9, 615-627.

4- S. K. Hobbs, W. L. Monsky, F. Yuan, W. G. Roberts, L. Griffith, V. P. Torchilin and R. K. Jain, *Proc. Natl. Acad. Sci U. S. A.*, **1998**, 95, 4607-4612.

5- S. Dhar, N. Kolishetti, S. J. Lippard and O. C. Farokhzad, *Proc. Natl. Acad. Sci. U. S. A.*, **2011**, 108, 1850-1855.

6- E. Mahon, A. Salvati, F. Baldelli Bombelli, I. Lynch and K. A. Dawson, *J. Control. Release*, **2012**, 161, 164-174.

7- A. Albanese, P. S. Tang and W. C.W. Chan, *Annu. Rev. Biomed. Eng*., **2012**, 14, 1–16.

8- M. Mahmoudi, I. Lynch, M. R. Ejtehadi, M. P. Monopoli, F. B. Bombelli and S. Laurent, *Chem. Rev.*, **2011**, 111, 5610-5637.

9- M. P. Monopoli, D. Walczyk, A. Campbell, G. Elia, I. Lynch, F. Baldelli Bombelli and K. A. Dawson, *J. Am. Chem. Soc.*, **2011**, 133, 2525-2534.

10- D. Walczyk, F. B. Bombelli, M. P. Monopoli, I. Lynch and K. A. Dawson, *J. Am. Chem. Soc.*, **2010**, 132, 5761-5768.

11- A. Lesniak, F. Fenaroli, M. P. Monopoli, C. A. berg, K. A. Dawson and A. Salvati, *ACS Nano*, **2012**, 6, 5845-5857.

12- A. Lesniak, A. Campbell, M. P. Monopoli, I. Lynch, A. Salvati and K. A. Dawson, *Biomaterials*, **2010**, 31, 9511-9518.

13- O. B. Garner and L.G. Baum, *Biochem. Soc. Trans.*, **2008**, 36, 1472-1477.

14- M. M. Fuster and J. D. Esko, *Nat. Rev. Cancer*, **2005**, 5, 526-542.

15- S. T. Laughlin, J. M. Baskin, S. L. Amacher and C. R. Bertozzi, *Science,* **2008**, 320, 664-667.

16- L. K. Mahal, K. J. Yarema and C. R. Bertozzi, *Science,* **1997**, 276, 1125-1128.

17- J. A. Prescher and C. R. Bertozzi, *Cell*, **2006**, 126, 851-854.

18- H. C. Kolb, M. G. Finn and K. B. Sharpless, *Angew. Chem. Int. Ed.*, **2001**, 40, 2004-2021.

19- J. C. Jewett and C. R. Bertozzi, *Chem. Soc. Rev.*, **2010**, 39, 1272–1279.

20- V. V. Rostovtsev, L. G. Green, V. V. Fokin and K. B. Sharpless, *Angew. Chem., Int. Ed.*, **2002**, 41, 2596–2599.

21- C. W. Tornøe, C. Christensen and M. Meldal, *J. Org. Chem.*, **2002**, 67, 3057–3064.

22- E. Saxon and C. R. Bertozzi, *Science*, **2000**, 287, 2007-2010.

23- M. J. Hangauer and C. R. Bertozzi, *Angew. Chem. Int. Ed.,* **2008**, 47, 2394-2397.

24- G. Wittig and A. Krebs, *I. Chem. Ber*., **1961**, 94, 3260-3275.

25- J. M. Baskin, J. A. Prescher, S. T. Laughlin, N. J. Agard, P. V. Chang, I. A. Miller, A. Lo, J. A. Codelli and C. R. Bertozzi, *Proc. Natl. Acad. Sci U. S. A.,* **2007***,* 104, 16793-16797.

26- P. V. Chang, J. A. Prescher, E. M. Sletten, J. M. Baskin, I. A. Miller, N. J. Agard, A. Lo and C. R. Bertozzi, *Proc. Natl. Acad. Sci U. S. A.,* **2010**, 107, 1821-1826.

27- J. Dommerholt, S. Schmidt, R. Temming, L. J. A. Hendriks, F. P. J. T. Rutjes, J. C. M. van Hest, D. J. Lefeber, P. Friedl and F. L. van Delft, *Angew. Chem. Int. Ed.*, **2010**, 49, 9422-9425.

28- S. J, Luchansky, H. C. Hang, E. Saxon, J. R. Grunwell, C. Yu, D. H. Dube and C. R. Bertozzi, *Methods Enzymol.*, **2003**, 362, 249-272.

29- L. Tang, T. M. Fan, L. B. Borst and J. Cheng, *ACS Nano*, **2012**, 6, 3954-3966.

30- X. Zhao, L. R. Hilliard, S. J. Mechery, Y. Wang, R. P. Bagwe, S. Jin and W. Tan, *Proc. Natl. Acad. Sci.U. S. A.*, **2004**, 101, 15027-15032.

31- J. C. Jewett, E. M. Sletten and Carolyn R. Bertozzi, *J. Am. Chem. Soc.,* **2004**, 132, 3688-3690.

32- V. Mirshafiee, M. Mahmoudi, K. Lou, J. Cheng and M. L. Kraft, *ChemComm.*, **2013**, 49, 2557-2559.

33- X. Gao, Y. Cui, R. M. Levenson, L. W. K. Chung and S. Nie, *Nat. Biotech.*, **2004**, 22, 969-976.

34- C. H. J. Choi, C. A. Alabi, P. Webster and M. E. Davis, *Proc. Natl. Acad. Sci U. S. A.*, **2010**, 107, 1235-1240.

35- G. Maiorano, S. Sabella, B. Sorce, V. Brunetti, M. A. Malvindi, R. Cingolani and P. P. Pompa, *ACS Nano*, **2010**, 4, 7481-7491.

36- Z. J. Deng, M. Liang, M. Monteiro, I. Toth and R. F. Minchin, *Nature Nanotech.*, **2011**, 6, 39-44.

37- N. Bertrand and J.-C. Leroux, *J. Control. Release*, **2012**, 161, 152-163.

38- B. D. Chithrani and W. C. W. Chan, *Nano Lett.*, **2007**, 7, 1542-1550.

39- M. A. Dobrovolskaia, P. Aggarwal, J. B. Hall and S. E. McNeil, *Mol. Pharm.*, **2008**, 5, 487-495.

40- Y.-S. Fu and S. J. Yu, *Angew. Chem. Int. Ed.*, **2001**, 40, 437-440.

41- M. L. Kraft and J. S. Moore, *Langmuir*, **2004**, 20, 1111-1119.

42- P. K. B. Palomaki and P. H. Dinolfo, *ACS Appl. Mater. Interfaces*, **2011**, 3, 4703-4713.

43- C. Radhakrishnan, M. K. F. Lo, M. V. Warrier, M. A. Garcia-Garibay and H. G. Monbouquette, *Langmuir*, **2006**, 22, 5018-5024.

44- K. Shapero, F. Fenaroli, I. Lynch, D. C. Cottell, A. Salvati and K. A. Dawson, *Mol. BioSyst.*, **2011**, 7, 371-378.

45- R. Gref, M. Lück, P. Quellec, M. Marchand, E. Dellacherie, S. Harnisch, T. Blunk and R. H. Müller, *Colloids Surf. B Biointerfaces*, **2000**, 18, 301-313.

46- M. Lundqvist, J. Stigler, T. Cedervall, T. Berggård, M. B. Flanagan, I. Lynch, G. Elia and K. Dawson, *ACS Nano*, **2011**, 5, 7503-7509.

47- M. Ghavami, S. Saffar, B. Abd Emamy, A. Peirovi, M. A. Shokrgozar, V. Serpooshan and M. Mahmoudi, *RSC Advances*, **2013**, 3, 1119-1126.

48- G. Caracciolo, D. Pozzi, A. L. Capriotti, C. Cavaliere, F. Cardarelli, A. Bifone, G. Bardi, F. Salomone and A. Laganà, Nanotechnology 2012, Santa Clara, CA, **2012**.